



Adducts of ruthenium(IV) thiolates with substituted pyridines. Syntheses and structures of $[\text{Ru}(\text{SMes})_4(\text{R-py})]$ ($\text{R} = 4\text{-Et}, 4\text{-}^t\text{Bu}, \text{and } 3,5\text{-Me}_2$) and $[\{\text{Ru}(\text{SMes})_4\}_2(\mu\text{-}4,4'\text{-bipy})]$ ($\text{Mes} = 2,4,6\text{-trimethylphenyl}$)

Xin Chen, Ai-Quan Jia, Rufei Ye, Hua-Tian Shi & Qian-Feng Zhang

To cite this article: Xin Chen, Ai-Quan Jia, Rufei Ye, Hua-Tian Shi & Qian-Feng Zhang (2015) Adducts of ruthenium(IV) thiolates with substituted pyridines. Syntheses and structures of $[\text{Ru}(\text{SMes})_4(\text{R-py})]$ ($\text{R} = 4\text{-Et}, 4\text{-}^t\text{Bu}, \text{and } 3,5\text{-Me}_2$) and $[\{\text{Ru}(\text{SMes})_4\}_2(\mu\text{-}4,4'\text{-bipy})]$ ($\text{Mes} = 2,4,6\text{-trimethylphenyl}$), Journal of Coordination Chemistry, 68:16, 2835-2845, DOI: [10.1080/00958972.2015.1061658](https://doi.org/10.1080/00958972.2015.1061658)

To link to this article: <http://dx.doi.org/10.1080/00958972.2015.1061658>



Accepted author version posted online: 15 Jun 2015.
Published online: 09 Jul 2015.



Submit your article to this journal [↗](#)



Article views: 31



View related articles [↗](#)



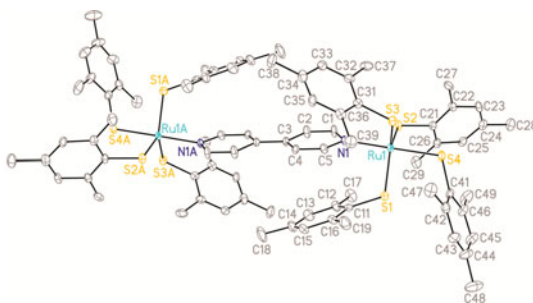
View Crossmark data [↗](#)

Adducts of ruthenium(IV) thiolates with substituted pyridines. Syntheses and structures of $[\text{Ru}(\text{SMes})_4(\text{R-py})]$ ($\text{R} = 4\text{-Et}$, $4\text{-}^t\text{Bu}$, and $3,5\text{-Me}_2$) and $[\{\text{Ru}(\text{SMes})_4\}_2(\mu\text{-}4,4'\text{-bipy})]$ ($\text{Mes} = 2,4,6\text{-trimethylphenyl}$)

XIN CHEN, AI-QUAN JIA, RUFEI YE, HUA-TIAN SHI and QIAN-FENG ZHANG*

Institute of Molecular Engineering and Applied Chemistry, Anhui University of Technology,
Ma'anshan, PR China

(Received 6 January 2015; accepted 6 May 2015)



Treatment of the trigonal-bipyramidal ruthenium(IV)–thiolate complex, $[\text{Ru}(\text{SMes})_4(\text{MeCN})]$ ($\text{Mes} = 2,4,6\text{-trimethylphenyl}$, **1**), with an anhydrous diethyl ether solution of hydrogen chloride in THF afforded $[\text{Ru}(\text{SMes})_3\text{Cl}(\text{MeCN})]$ (**2**), whereas interaction of **1** with $[\text{Et}_4\text{N}]\text{Cl}$ in THF gave an anionic ruthenium(IV)–thiolate complex, $[\text{Et}_4\text{N}][\text{Ru}(\text{SMes})_4\text{Cl}]$ (**3**). Reaction of **1** with one equivalent of substituted pyridines in dichloromethane gave the corresponding pyridine-coordinated ruthenium(IV)–thiolate complexes, $[\text{Ru}(\text{SMes})_4(\text{R-py})]$ ($\text{R} = 4\text{-Et}$, **4**; $4\text{-}^t\text{Bu}$, **5**; $3,5\text{-Me}_2$, **6**), while reaction of **1** with 0.5 equiv. of $4,4'\text{-bipy}$ ($4,4'\text{-bipy} = 4,4'\text{-bipyridine}$) in dichloromethane resulted in the formation of a dinuclear ruthenium(IV)–thiolate complex $[\{\text{Ru}(\text{SMes})_4\}_2(\mu\text{-}4,4'\text{-bipy})]$ (**7**). Complexes **2–7** have been spectroscopically characterized along with their electrochemical analyses, and their structures have been determined by single-crystal X-ray diffraction.

Keywords: Ruthenium complex; Pyridine; Thiolate; Synthesis; Crystal structure

1. Introduction

The chemistry of transition metals coordinated to sulfur-donors is well exploited in both industry and biology [1–3]. Thiolate complexes are possibly relevant to the structures, bonding, and functions of active centers in metalloproteins such as ferredoxins, nitrogenases,

*Corresponding author. Email: zhangqf@ahut.edu.cn

and metallothioneins [4]. Coordinatively unsaturated metal–sulfur centers located on the surfaces and edges of metal sulfide crystallites have been proposed to be the active sites of metal sulfur heterogeneous catalysts [5]. Specifically, RuS₂ is a very active catalyst for the industrially important hydrodesulfurization reaction [6, 7]. In these applications, sulfur-coordination is necessary for the functionization of the metal sulfide active centers. In contrast to the considerable chemistry of iron–thiolate and iron–sulfide–thiolate complexes, the chemistry of ruthenium thiolate complexes has been less extensively developed. While ruthenium(II) thiolate complexes are well documented, for example, [$\{\text{Ru}(\mu\text{-SR})(\text{SCNMe}_2)(\text{CO})(\text{PPh}_3)\}(\text{NO}_3)_n$] (R = Ph, Et; n = 0, 4) is typical ruthenium(II) thiolate complexes of which the complex with R = Ph was found to exhibit a four-electron transfer, which is important for the reduction of O₂ to H₂O in fuel cells [8], the analogous ruthenium(IV) systems have received less attention [9–13]. Millar and Koch first reported the trigonal-bipyramidal ruthenium(IV) complexes [Ru(SAr)₄(MeCN)] (Ar = 2,3,5,6-tetramethylphenyl, 2,4,6-triisopropylphenyl) in which the labile MeCN was easily substituted by CO to form [Ru(SAr)₄(CO)] [14, 15]. We have previously reported σ -acetylide complexes of ruthenium(IV) thiolates [Et₃NH][Ru(SXyl)₃(C \equiv CPh)Cl] (Xyl = 2,6-dimethylphenyl), obtained by reaction of [Ru(SXyl)₃(MeCN)Cl] with PhC \equiv CH in the presence of NEt₃ [16]. In more recent work, using [Ru(SMes)₄(MeCN)], we extended these reactions to alkynols HC \equiv CCR₂OH (R = Me, Et), resulting in the isolation of thiolato-bridged dinuclear ruthenium(IV) vinyl complexes [17]. As part of our long-standing interest in high-valent ruthenium complexes with aryl-thiolate ligands, we are currently interested in new adducts of ruthenium(IV) thiolates with substituted pyridines. Herein, we report the syntheses and structures of the mononuclear ruthenium(IV)–thiolate complexes [Ru(SMes)₄(R-py)] (R = 4-Et, 4-^tBu and 3,5-Me₂) and the dinuclear ruthenium(IV)–thiolate complex [$\{\text{Ru}(\text{SMes})_4\}_2(\mu\text{-4,4'-bipy})$], which are expected to expand the pool of ruthenium(IV)–thiolate complexes for the comparative study of their molecular structures and spectroscopic properties.

2. Experimental

2.1. General considerations

All synthetic manipulations were carried out under dry nitrogen using standard Schlenk techniques. 4-Ethyl-pyridine, 4-*tert*-butyl-pyridine, 3,5-dimethyl-pyridine, and 4,4'-bipyridine were purchased from Alfa Aesar Ltd and used without purification. [Ru(SMes)₄(MeCN)] (**1**) was prepared according to the literature method [17]. NMR spectra were recorded on a Bruker ALX 400 Plus spectrometer operating at 400 MHz for ¹H. Chemical shifts (δ , ppm) were reported with reference to SiMe₄. Infrared spectra (KBr) were recorded on a Perkin–Elmer 16 PC FT-IR spectrophotometer as KBr pellets, and positive FAB mass spectra were recorded on a Finnigan TSQ 7000 spectrometer. Cyclic voltammetry was performed with a CHI 660 electro-chemical analyzer. A standard three-electrode cell was used with glassy carbon working electrode, platinum counter electrode, and Ag/AgCl reference electrode under nitrogen at 25 °C. Formal potentials (E^0) were measured in CH₂Cl₂ solutions with 0.1 M [ⁿBu₄N]PF₆ as the supporting electrolyte and reported with reference to the ferrocene–ferrocene couple (Cp₂Fe⁺⁰). In the –0.5 to +1.2 V region, a potential scan rate of 100 mV s^{–1} was used. Elemental analyses were carried out using a Perkin–Elmer 2400 CHN analyzer.

2.2. Synthesis of [Ru(SMes)₃Cl(MeCN)] (2)

To **1** (138 mg, 0.185 mmol) in THF (20 mL) was added HCl (2.32 mL of a 1.5 M solution in Et₂O), and the mixture was stirred for 4 h at room temperature. The solvent was removed under vacuum, and the residue was washed with Et₂O and hexane. Recrystallization from CH₂Cl₂/Et₂O (1:3) afforded a brown crystalline solid of **2**. Yield: 84 mg, 72%. IR (KBr disk): $\nu(\text{C}\equiv\text{N})$ 2231 (*vs.*), $\nu(\text{C}-\text{S})$ 796 (m) and 643 (m) cm⁻¹. ¹H NMR (CDCl₃): δ 1.96 (s, 3H, CH₃CN), 2.32 (s, 9H, CH₃), 2.64 (s, 18H, CH₃), 6.65 (t, *J* = 7.4 Hz, 2H, *H_p*), 6.97 (t, *J* = 7.2 Hz, 6H, *H_p*). MS (FAB): *m/z* 632 [*M*⁺ + 1], 589 [Ru(SMes)₃Cl], 554 [Ru(SMes)₃], 402 [Ru(SMes)₂]. Anal. Calcd for C₂₉H₃₆NCIS₃Ru: C, 55.17; H, 5.75; N, 2.22%. Found: C, 55.12; H, 5.74; N, 2.20%.

2.3. Synthesis of [Et₄N][Ru(SMes)₄Cl] (3)

To **1** (138 mg, 0.185 mmol) in THF (20 mL) was added [Et₄N]Cl (31 mg, 0.185 mmol), and the mixture was stirred for 4 h at room temperature. The solvent was removed under vacuum, and the residue was washed with Et₂O. Recrystallization from CH₂Cl₂/Et₂O (1:3) afforded a brown-red crystalline solid of **3**. Yield: 51 mg, 92%. IR (KBr disk): $\nu(\text{C}-\text{S})$ 792 (m) and 657 (m) cm⁻¹. ¹H NMR (CDCl₃): δ 1.29 (t, 12H, CH₂CH₃), 2.02 (s, 6H, PhCH₃), 2.08 (s, 3H, PhCH₃), 2.15 (s, 12H, PhCH₃), 2.31 (s, 12H, PhCH₃), 2.47 (s, 12H, PhCH₃), 3.31 (dt, 8H, CH₂CH₃), 6.12 (t, *J* = 7.4 Hz, 4H, *H_p*), 6.64 (t, *J* = 7.2 Hz, 4H, *H_p*), 6.93 (t, *J* = 7.4 Hz, 4H, *H_p*). MS (FAB): *m/z* 872 [*M*⁺ + 1], 741 [Ru(SMes)₄Cl], 554 [Ru(SMes)₃], 402 [Ru(SMes)₂]. Anal. Calcd for C₄₄H₆₄NCIS₄Ru: C, 60.62; H, 7.40; N, 1.61%. Found: C, 60.53; H, 7.44; N, 1.58%.

2.4. Synthesis of [Ru(SMes)₄(4-Etpy)] (4)

A mixture of **1** (138 mg, 0.185 mmol) and 4-Etpy (20 mg, 0.185 mmol) in dichloromethane (10 mL) was stirred for 4 h at room temperature. During this time, the solution changed from brown to dark red. The solvent was removed under vacuum, and the residue was washed with Et₂O and hexane. Recrystallization from CH₂Cl₂/Et₂O (1:4) gave dark red block-shaped crystals of **4**. Yield: 51 mg, 69%. IR (KBr disk): $\nu(\text{C}=\text{N})$ 1614 (s) and 1583 (s), $\nu(\text{C}-\text{S})$ 781 (m) and 647 (m) cm⁻¹. ¹H NMR (CDCl₃): δ 1.21 (s, 3H, CH₂CH₃), 2.03 (s, 6H, PhCH₃), 2.06 (s, 3H, PhCH₃), 2.19 (s, 12H, PhCH₃), 2.32 (s, 12H, PhCH₃), 2.45 (s, 12H, PhCH₃), 2.61 (t, *J* = 5.2 Hz, 2H, CH₂CH₃), 6.19 (t, *J* = 7.4 Hz, 4H, *H_p*), 6.63 (t, *J* = 7.2 Hz, 4H, *H_p*), 6.97 (t, *J* = 7.4 Hz, 4H, *H_p*), 7.28 (d, *J* = 5.8 Hz, 2H, *H_o* in *py*), 8.51 (d, *J* = 6.2 Hz, 2H, *H_m* in *py*). MS (FAB): *m/z* 832 [*M*⁺ + 1], 706 [Ru(SMes)₄], 554 [Ru(SMes)₃], 402 [Ru(SMes)₂]. Anal. Calcd for C₄₃H₅₃NS₄Ru: C, 63.51; H, 6.57; N, 1.72%. Found: C, 63.43; H, 6.54; N, 1.70%.

2.5. Synthesis of [Ru(SMes)₄(4^{-t}Bupy)] (5)

The method was similar to that used for **4**, employing 4^{-t}Bupy (25 mg, 0.185 mmol) instead of 4-Etpy. Recrystallization from CH₂Cl₂/Et₂O (1:5) gave dark red block-shaped crystals of **5**. Yield: 102 mg, 74%. IR (KBr disk): $\nu(\text{C}=\text{N})$ 1619 (s) and 1581 (s), $\nu(\text{C}-\text{S})$ 776 (m) and 653 (m) cm⁻¹. ¹H NMR (CDCl₃): δ 2.06 (s, 6H, PhCH₃), 2.09 (s, 3H, PhCH₃), 2.19 (s, 12H, PhCH₃), 2.27 (s, 12H, PhCH₃), 2.45 (s, 12H, PhCH₃), 6.18 (t, *J* = 7.4 Hz, 4H, *H_p*),

6.61 (t, $J = 7.2$ Hz, 4H, H_p), 6.93 (t, $J = 7.4$ Hz, 4H, H_p), 7.39 (d, $J = 6.0$ Hz, 2H, H_o in py), 8.48 (d, $J = 6.0$ Hz, 2H, H_m in py). MS (FAB): m/z 841 [M^+], 706 [Ru(SMes)₄], 554 [Ru(SMes)₃], 402 [Ru(SMes)₂]. Anal. Calcd for C₄₅H₅₇NS₄Ru: C, 64.24; H, 6.83; N, 1.66%. Found: C, 64.21; H, 6.76; N, 1.68%.

2.6. Synthesis of [Ru(SMes)₄(3,5-Me₂py)] (6)

The method was similar to that used for **4**, employing 3,5-Me₂py (20 mg, 0.185 mmol) instead of 4-Etpy. Recrystallization from CH₂Cl₂/Et₂O (1:4) gave dark red block-shaped crystals of **6**. Yield: 109 mg, 76%. IR (KBr disk): $\nu(C=N)$ 1624 (s) and 1589 (s), $\nu(C-S)$ 782 (m) and 659 (m) cm⁻¹. ¹H NMR (CDCl₃): δ 1.24 (s, 9H, CH₃ in ^tBu), 2.01 (s, 6H, PhCH₃), 2.07 (s, 3H, PhCH₃), 2.17 (s, 12H, PhCH₃), 2.29 (s, 12H, PhCH₃), 2.48 (s, 12H, PhCH₃), 2.53 (s, 3H, CH₃ in py), 2.56 (s, 3H, CH₃ in py), 6.15 (t, $J = 7.4$ Hz, 4H, H_p), 6.59 (t, $J = 7.2$ Hz, 4H, H_p), 6.91 (t, $J = 7.4$ Hz, 4H, H_p), 7.44 (d, $J = 5.8$ Hz, 2H, H_o in py), 8.79 (d, $J = 6.0$ Hz, 1H, H_p in py). MS (FAB): m/z 813 [M^+], 706 [Ru(SMes)₄], 554 [Ru(SMes)₃], 402 [Ru(SMes)₂]. Anal. Calcd for C₄₃H₅₃NS₄Ru: C, 63.51; H, 6.57; N, 1.72%. Found: C, 63.47; H, 6.55; N, 1.71%.

2.7. Synthesis of [Ru(SMes)₄]₂(μ -4,4'-bipy)] (7)

To a solution of **1** (138 mg, 0.185 mmol) in CH₂Cl₂ (20 mL) was added 4,4'-bipy (31 mg, 0.185 mmol) in CH₂Cl₂ (5 mL), and the mixture was stirred for 2 h at room temperature. The solvent was removed under vacuum, and the residue was washed with Et₂O. Recrystallization from CH₂Cl₂/Et₂O (1:3) afforded dark red crystals of **7**. Yield: 51 mg, 92%. IR (KBr disk): $\nu(C=N)$ 1636 (s) and 1591 (s), $\nu(C-S)$ 785 (m) and 662 (m) cm⁻¹. ¹H NMR (CDCl₃): δ 2.05 (s, 12H, PhCH₃), 2.11 (s, 6H, PhCH₃), 2.19 (s, 24H, PhCH₃), 2.27 (s, 24H, PhCH₃), 2.51 (s, 24H, PhCH₃), 6.13 (t, $J = 7.4$ Hz, 8H, H_p), 6.53 (t, $J = 7.2$ Hz, 8H, H_p), 6.97 (t, $J = 7.4$ Hz, 8H, H_p), 7.38 (d, $J = 6.6$ Hz, 2H, H_o in py), 7.58 (d, $J = 6.8$ Hz, 2H, H_p in py). MS (FAB): m/z 1568 [M^+], 706 [Ru(SMes)₄], 554 [Ru(SMes)₃], 402 [Ru(SMes)₂]. Anal. Calcd for C₈₂H₉₆N₂S₈Ru₂: C, 62.80; H, 6.17; N, 1.79%. Found: C, 62.83; H, 6.15; N, 1.81%.

2.8. X-ray diffraction measurements

Crystallographic data and experimental details for [Ru(SMes)₃Cl(MeCN)] (**2**), [Et₄N][Ru(SMes)₄Cl] (**3**), [Ru(SMes)₄(4-Etpy)] (**4**), [Ru(SMes)₄(4-^tBupy)] (**5**), [Ru(SMes)₄(3,5-Me₂py)] (**6**), and [Ru(SMes)₄]₂(μ -4,4'-bipy)] (**7**) are summarized in table 1. Selected bond lengths and angles are compiled in table 2 for comparison. Intensity data were collected on a Bruker SMART APEX 2000 CCD diffractometer using graphite-monochromated Mo-K α radiation ($\lambda = 0.71073$ Å) at 293(2) K. The collected frames were processed with SAINT [18]. The data were corrected for absorption using SADABS [19]. Structures were solved by the direct methods and refined by full-matrix least-squares on F^2 using the SHELXTL software package [20, 21]. All non-hydrogen atoms except for the lattice solvent molecules were refined anisotropically. The positions of all hydrogens were generated geometrically ($C_{sp3}-H = 0.96$ and $C_{sp2}-H = 0.93$ Å), assigned isotropic thermal parameters, and allowed to ride on their respective parent carbon or nitrogen before the final cycle of least-squares refinement.

Table 1. Crystallographic data and experimental details for [Ru(SMes)₅Cl(MeCN)] (2), [Et₄N][Ru(SMes)₄(4-Et₃py)] (4), [Ru(SMes)₄(4-Et₃py)] (5), [Ru(SMes)₄(3,5-Me₂py)] (6), and [Ru(SMes)₄(*tt*-4,4'-bipy)] (7).

Compound	2	3	4	5	6	7
Empirical formula	C ₂₉ H ₃₆ NClS ₃ Ru	C ₄₄ H ₆₄ NClS ₄ Ru	C ₄₃ H ₅₃ NS ₄ Ru	C ₄₅ H ₅₇ NS ₄ Ru	C ₄₃ H ₅₃ NS ₄ Ru	C ₃₂ H ₄₆ N ₂ S ₈ Ru ₂
Formula weight	631.29	871.72	813.17	841.23	813.17	1568.23
Crystal system	Monoclinic	Monoclinic	Monoclinic	Orthorhombic	Monoclinic	Triclinic
<i>a</i> (Å)	15.394(4)	11.744(2)	12.8660(11)	14.5529(12)	17.687(5)	14.184(3)
<i>b</i> (Å)	11.399(3)	19.007(3)	19.3823(17)	17.2292(15)	11.908(4)	16.674(4)
<i>c</i> (Å)	18.203(5)	21.779(4)	16.6500(13)	19.0867(16)	20.680(7)	19.418(7)
α (°)						
β (°)	107.238(6)	91.491(4)	97.913(2)		100.871(8)	98.226(8)
γ (°)						111.722(6)
<i>V</i> (Å ³)	3050.8(15)	4859.8(14)	4112.5(6)	4785.7(7)	4277(2)	4081(2)
Space group	<i>P</i> 2 ₁ / <i>n</i>	<i>P</i> 2 ₁ / <i>n</i>	<i>P</i> 2 ₁ / <i>n</i>	<i>P</i> 2 ₁ 2 ₁ 2 ₁	<i>P</i> 2 ₁ / <i>c</i>	<i>P</i> -1
<i>Z</i>	4	4	4	4	4	2
<i>D</i> _{calc} (g cm ⁻³)	1.374	1.204	1.313	1.168	1.263	1.276
Temperature (K)	296(2)	296(2)	296(2)	296(2)	296(2)	296(2)
<i>F</i> (0 0 0)	1304	1840	1704	1768	1704	1636
μ (Mo-K α) (mm ⁻¹)	0.825	0.577	0.614	0.530	0.591	0.616
Total refin	19,459	30,696	26,605	31,177	27,322	22,826
Independent refin	6900	10,982	9373	10,633	9508	14,157
Parameters	326	476	455	475	456	847
<i>R</i> _{int}	0.0811	0.0422	0.0355	0.0356	0.1016	0.0498
<i>R</i> 1 ^a , <i>wR</i> 2 ^b [<i>I</i> > 2 σ (<i>I</i>)]	0.0798, 0.0973	0.0699, 0.1887	0.0366, 0.0881	0.0422, 0.1088	0.0815, 0.1283	0.0660, 0.1801
<i>R</i> 1, <i>wR</i> 2 (all data)	0.0858, 0.1248	0.1114, 0.2125	0.0628, 0.1036	0.0663, 0.1260	0.1065, 0.1632	0.1261, 0.2184
GoF ^c	0.892	0.958	1.009	1.049	0.977	0.894

^a $R1 = \|F_o\| - |F_c| / \|F_o\|$ ^b $wR2 = [w(F_o^2 - F_c^2) / w(F_o^2)]^{1/2}$ ^cGoF = $[w(F_o^2 - F_c^2) / (N_{obs} - N_{param})]^{1/2}$

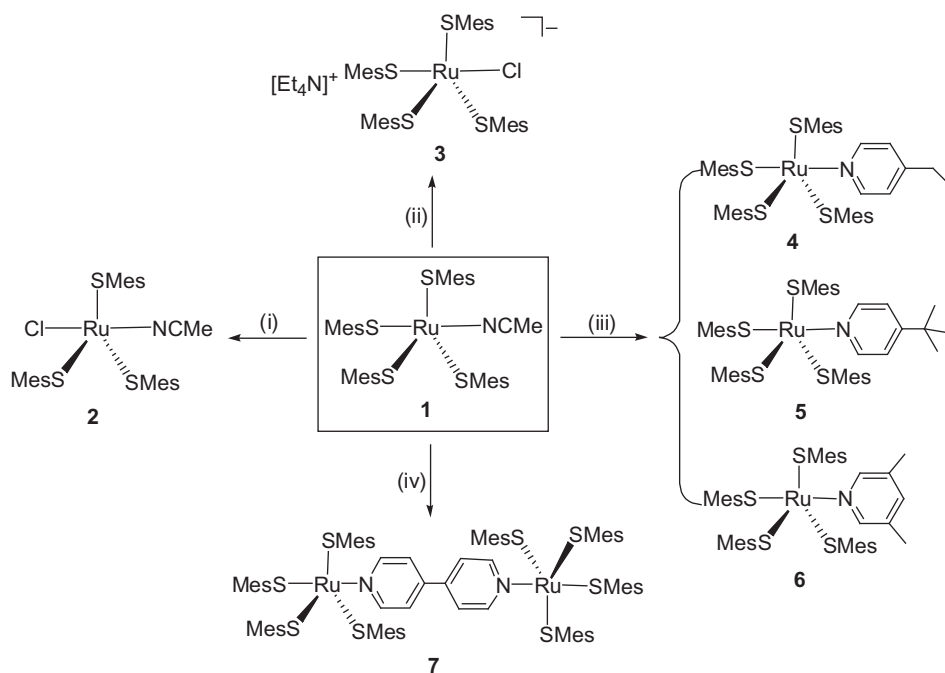
Table 2. Selected bond lengths (Å) and angles (°) for **2–7**.

Complex	Ru–N	Ru–S _{eq}	Ru–S _{ax}	Ru–Cl	Cl/S–Ru–N	S–Ru–S
[Ru(SMes) ₃ Cl(MeCN)] 2	2.009(5)	2.197(2) 2.203(2) 2.203(2)		2.3655(17)	177.39(17)	117.70(8) 119.50(9) 122.78(9)
[Et ₄ N][Ru(SMes) ₄ Cl] 3		2.1999(15) 2.2058(15) 2.2014(15)	2.4125(14)	2.4475(13)	178.16(5)	115.51(7) 122.97(6) 121.27(7)
[Ru(SMes) ₄ (4-Etpy)] 4	2.180(2)	2.2127(7) 2.1989(7) 2.2041(7)	2.3997(7)		176.89(6)	120.50(3) 124.66(3) 114.53(3)
[Ru(SMes) ₄ (4- ^t Bupy)] 5	2.208(3)	2.2142(10) 2.2027(11) 2.2027(11)	2.4042(10)		177.28(9)	117.40(3) 124.05(4) 118.30(5)
[Ru(SMes) ₄ (3,5-Me ₂ py)] 6	2.179(6)	2.202(2) 2.2021(18) 2.2106(16)	2.4221(19)		178.52(16)	116.45(7) 123.86(7) 119.49(8)
[{Ru(SMes) ₄ } ₂ (μ-4,4'-bipy)] 7	2.182(5)	2.203(2) 2.188(2) 2.199(2)	2.3808(19)		178.10(17)	120.37(9) 123.10(9) 116.24(9)

3. Results and discussion

Interaction of the trigonal-bipyramidal ruthenium(IV)–thiolate complex [Ru(SMes)₄(MeCN)] (**1**) in THF and an anhydrous solution of hydrogen chloride in diethyl ether at room temperature for 4 h followed by recrystallization from CH₂Cl₂/Et₂O at room temperature afforded [Ru(SMes)₃Cl(MeCN)] (**2**) as the sole isolable product (scheme 1). The axial arene-thiolate ligand in the starting ruthenium material was substituted by one chloride, indicating that the axial thiolate could be selectively replaced [22]. Previously, [Ru(SXyl)₃Cl(MeCN)] was obtained by an analogous procedure [16]. Reaction of **1** with [Et₄N]Cl in THF at room temperature gave an anionic ruthenium(IV)–thiolate complex [Et₄N][Ru(SMes)₄Cl] (**3**) only. Obviously, the labile MeCN ligand dissociated, and one chloride coordinated to the ruthenium(IV) center to result in **3**. A similar complex [Et₄N][Ru(SXyl)₄Cl] was reported as a minor product of the reaction of [Et₄N][RuCl₄(MeCN)₂] and XylSH in the presence of sodium methoxide [16]. Treatment of **1** with 1 equiv. of three different substituted pyridines resulted in isolation of corresponding pyridine-coordinated Ru(IV) complexes, [Ru(SMes)₄(R-py)] (R = 4-Et, **4**; 4-^tBu, **5**; 3,5-Me₂, **6**). The reaction involved the substitution of the labile MeCN moiety by pyridine ligands. Reaction of **1** with 0.5 equiv. of 4,4'-bipy (4,4'-bipy = 4,4'-bipyridine) in dichloromethane gave the expected dinuclear Ru(IV) thiolate complex [{Ru(SMes)₄}₂(μ-4,4'-bipy)] (**7**), in which the 4,4'-bipy a bridging ligand to link two [Ru(SMes)₄] species.

Complex **2** shows an infrared absorption at 2236 cm⁻¹ ascribed to the C≡N stretch. The characteristic bands for the pyridine-coordinated ruthenium(IV)–thiolate complexes **4–7** are 1614–1636 and 1581–1591 cm⁻¹ in the IR spectra, assignable to C=N and C–N bonds. Complexes **2–7** show C–S infrared absorption bands near 780 cm⁻¹ [17, 23]. The ¹H NMR spectrum of **2** shows the proton resonance of MeCN at 1.96 ppm as a singlet, shifted downfield compared to that in [Ru(SMes)₄(MeCN)] (1.93 ppm) [17]. The ¹H NMR spectra of **4**, **5**, and **7** display the pyridine proton resonances as two groups of doublets with the integration ratio of 1:1. The positive ion FAB mass spectra of **2–7** display the expected peaks corresponding to molecular ions [(M⁺) or (M⁺ + 1) or [Ru(SMes)₄] or [Ru(SMes)₃], or [Ru(SMes)₂] with the characteristic isotopic distribution patterns.



Scheme 1. Reactions of the ruthenium(IV)-thiolate complex $[\text{Ru}(\text{SMes})_4(\text{MeCN})]$. Reagents and conditions: (i) HCl in Et_2O , THF, room temperature (r.t.); (ii) $[\text{Et}_4\text{N}]\text{Cl}$, THF, r.t.; (iii) the substituted pyridines: 4-Etpy, 4-^tBupy, and 3,5-Me₂py, CH_2Cl_2 , r.t.; and (iv) 4,4'-bipy, CH_2Cl_2 , r.t.

The structures of $[\text{Ru}(\text{SMes})_3\text{Cl}(\text{MeCN})]$ (**2**), $[\text{Et}_4\text{N}][\text{Ru}(\text{SMes})_4\text{Cl}]$ (**3**), $[\text{Ru}(\text{SMes})_4(4\text{-Etpy})]$ (**4**), $[\text{Ru}(\text{SMes})_4(4\text{-}^t\text{Bupy})]$ (**5**), $[\text{Ru}(\text{SMes})_4(3,5\text{-Me}_2\text{py})]$ (**6**), and $[\{\text{Ru}(\text{SMes})_4\}_2(\mu\text{-}4,4'\text{-bipy})]$ (**7**) have been established by X-ray crystallography. All the ruthenium(IV)-thiolate complexes have trigonal-bipyramidal geometry (figures 1–6) [24]. The $\text{S}_{\text{eq}}\text{-Ru-S}_{\text{eq}}$ angles, from $114.53(3)^\circ$ to $124.66(3)^\circ$ in **2–7**, are all near 120° , while the axial

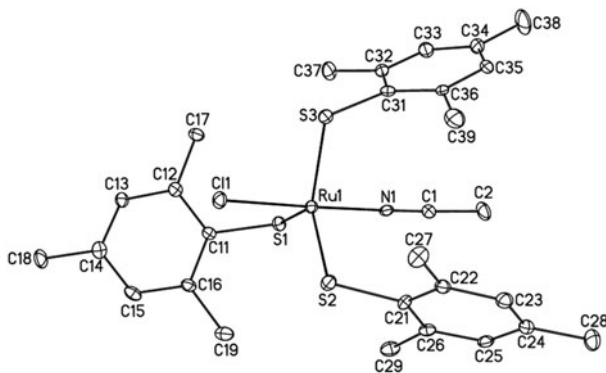


Figure 1. Molecular structure of $[\text{Ru}(\text{SMes})_3\text{Cl}(\text{MeCN})]$ **2**. Thermal ellipsoids are shown at the 40% probability level.

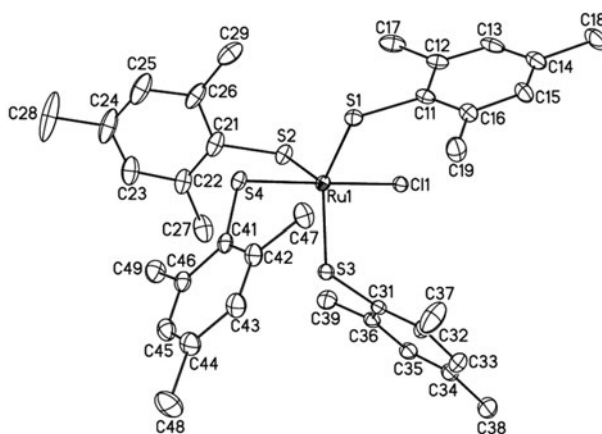


Figure 2. Molecular structure of $[\text{Ru}(\text{SMes})_4\text{Cl}]^-$ in **3**. Thermal ellipsoids are shown at the 40% probability level.

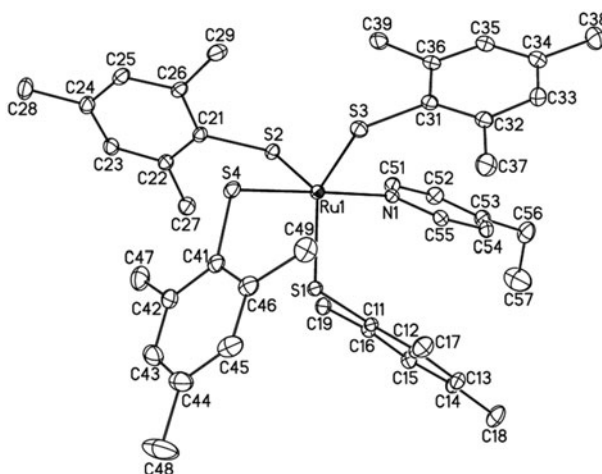


Figure 3. Molecular structure of **4**. Thermal ellipsoids are shown at the 40% probability level.

bond angles of Cl–Ru–N in **2** ($177.39(17)^\circ$), Cl–Ru–S_{ax} in **3** ($178.16(5)^\circ$), and S_{ax}–Ru–N in **4–7** ($176.89(6)^\circ$, $177.28(9)^\circ$, $178.52(16)^\circ$, $178.10(17)^\circ$) are all near 180° . The Ru–S_{ax} bond length ($\sim 2.40 \text{ \AA}$) is almost 0.2 \AA longer than the Ru–S_{eq} bond length ($\sim 2.20 \text{ \AA}$) in **3–7**, similar to that observed in $[\text{Ru}(\text{SAr})_4(\text{MeCN})]$ (Ar = 2,3,5,6-tetramethylphenyl) [14]. The Ru–Cl bond length of $2.3655(17) \text{ \AA}$ in $[\text{Ru}(\text{SMes})_3\text{Cl}(\text{MeCN})]$ (**2**) is little shorter than that of $2.4475(13) \text{ \AA}$ in $[\text{Et}_4\text{N}][\text{Ru}(\text{SMes})_4\text{Cl}]$ (**3**). The Ru–N(MeCN) bond length of $2.009(5) \text{ \AA}$ in **2** is comparable to that of $2.037(2) \text{ \AA}$ in a similar Ru(IV) complex $[\text{Ru}(\text{SXyl})_3\text{Cl}(\text{MeCN})]$ [16]. The Ru–N(pyridine) bond lengths from $2.179(6)$ to $2.208(3) \text{ \AA}$ in **4–7** are longer than those in related ruthenium(II) complexes $[(\text{NH}_3)\text{Ru}(\mu\text{-py}^{\text{si}}\text{S}_4)\text{Ru}(\text{py}^{\text{si}}\text{S}_4)]$ ($\text{py}^{\text{si}}\text{S}_4^{2-} = 2,6\text{-bis}(3\text{-triphenylsilyl-2-sulfanylphenylthiomethyl})\text{-pyridine}^{2-}$) ($2.064(3)$ and $2.030(3) \text{ \AA}$) [25], but comparable to those in the ruthenium(II)-pyridine complexes $[\text{Ru}(\text{py})(\text{PPh}_3)(\text{tpS}_4)]$ ($\text{tpS}_4^{2-} = 1,2\text{-bis}(2\text{-mercapto-phenylthio})\text{phenylene}^{2-}$) ($2.155(2) \text{ \AA}$) [26] and

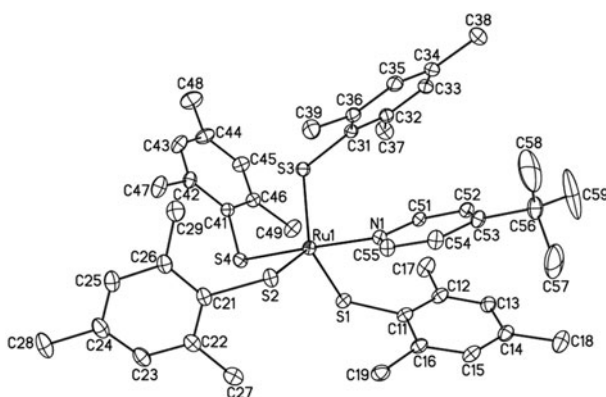


Figure 4. Molecular structure of **5**. Thermal ellipsoids are shown at the 40% probability level.

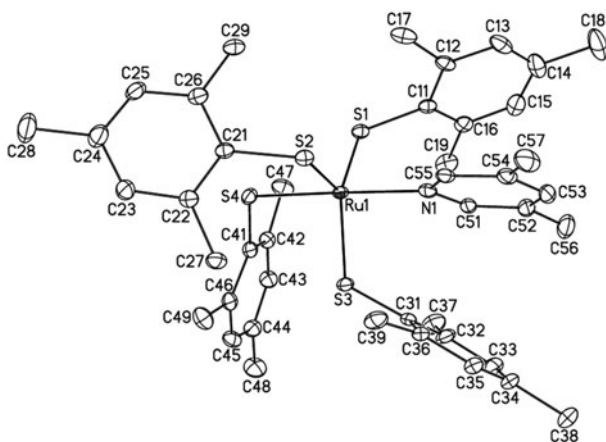


Figure 5. Molecular structure of **6**. Thermal ellipsoids are shown at the 40% probability level.

(BiBzIm = 2,2'-bisbenzimidazolate) (2.131(3) and 2.139 Å) [27]. The two pyridine rings of 4,4'-bipy in **7** are nearly coplanar. The separation of the two ruthenium bridged by 4,4'-bipy in **7** [av. 11.42(2) Å] is slightly longer than those in $[\text{Ru}_4(\eta^6\text{-C}_6\text{Me}_6)_4(\text{bpy})_2(\text{BiBzIm})_2]^{4+}$ (11.27 Å) [27], $[\{(\eta^6\text{-p-cymene})\text{Ru}\}_4(\mu\text{-OH})_4(\mu\text{-4,4'-bipy})_2][\text{BF}_4]_4$ [av. 11.30(1) Å] [28], and $[\{(\eta^6\text{-p-cymene})\text{Ru}\}_2(\mu\text{-C}_2\text{O}_4)_2(\mu\text{-4,4'-bipy})_2][\text{CF}_3\text{SO}_3]_4$ [11.32(1) Å] [29].

The formal potentials (E^0) of the ruthenium(IV)–thiolate complexes have been determined by cyclic voltammetry in dichloromethane, and the electrochemical data are summarized in table 3. The cyclic voltammograms of **1–7** in CH_2Cl_2 show a reversible couple at ca. -1.02 to -1.17 V, versus $\text{Cp}_2\text{Fe}^{+/0}$, which is assigned as the metal-centered $\text{Ru}^{\text{IV}}\text{–Ru}^{\text{III}}$ couple because the organic thiolate ligand is redox inactive at this potential, suggesting that E^0 is rather insensitive to L in $[\text{Ru}(\text{SMes})_4\text{L}]$. The E^0 for **7** is almost the same as those for the mononuclear **4–6**, indicating that there is negligible electronic communication between the two ruthenium(VI) centers in **7**.

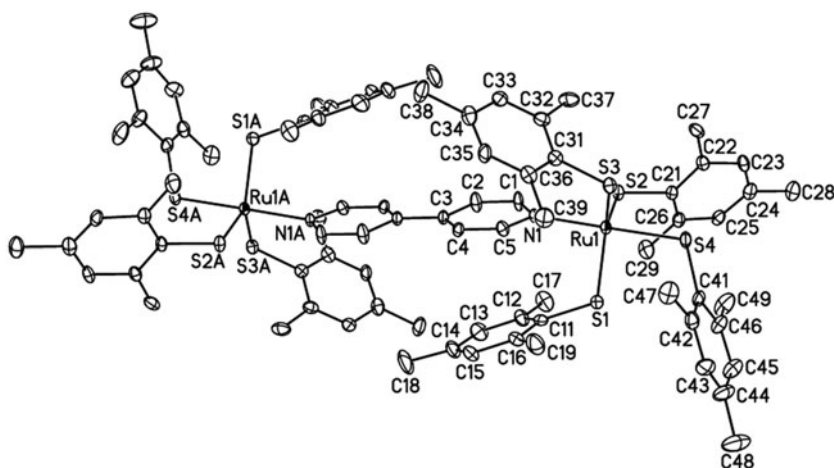


Figure 6. Molecular structure of $[\{\text{Ru}(\text{SMes})_4\}_2(\mu\text{-}4,4'\text{-bipy})]$ **7**. Thermal ellipsoids are shown at the 40% probability level.

Table 3. Formal potentials (E^0) for **1**–**7**.

Complex	E^0/V vs. ferrocene-ferrocenium, Ru(IV/III)
$[\text{Ru}(\text{SMes})_4(\text{MeCN})]$ 1	−1.10
$[\text{Ru}(\text{SMes})_3\text{Cl}(\text{MeCN})]$ 2	−1.21
$[\text{Et}_4\text{N}][\text{Ru}(\text{SMes})_4\text{Cl}]$ 3	−1.17
$[\text{Ru}(\text{SMes})_4(4\text{-Etpy})]$ 4	−1.02
$[\text{Ru}(\text{SMes})_4(4\text{-Bupy})]$ 5	−1.05
$[\text{Ru}(\text{SMes})_4(3,5\text{-Me}_2\text{py})]$ 6	−1.06
$[\{\text{Ru}(\text{SMes})_4\}_2(\mu\text{-}4,4'\text{-bipy})]$ 7	−1.09

In summary, treatment of the trigonal-bipyramidal ruthenium(IV)–thiolate complex $[\text{Ru}(\text{SMes})_4(\text{MeCN})]$ (**1**) in THF with an anhydrous diethyl ether solution of hydrogen chloride afforded $[\text{Ru}(\text{SMes})_3\text{Cl}(\text{MeCN})]$ (**2**) with the axial arene-thiolato ligand substituted by a chloride. The ionic ruthenium(IV)–thiolate complex $[\text{Et}_4\text{N}][\text{Ru}(\text{SMes})_4\text{Cl}]$ (**3**) was achieved by an alternate method using Et_4NCl with an improved yield [16]. Reaction of **1** with 1 equiv. of a substituted pyridine in dichloromethane gave the corresponding pyridine-coordinated Ru(IV) complexes **4**–**6** in good yields, which indicate a stronger interaction between the ruthenium center and the pyridine ligands. The isolation of the 4,4'-bipy bridged dinuclear ruthenium(IV)–thiolate complex $[\{\text{Ru}(\text{SMes})_4\}_2(\mu\text{-}4,4'\text{-bipy})]$ (**7**) confirmed the 4,4'-bipy substitution reaction. Further reactivity studies of ruthenium(IV)–thiolate complexes with other π -acid ligands are being carried out in this laboratory.

Supplementary material

Crystallographic data for $[\text{Ru}(\text{SMes})_3\text{Cl}(\text{MeCN})]$ (**2**), $[\text{Et}_4\text{N}][\text{Ru}(\text{SMes})_4\text{Cl}]$ (**3**), $[\text{Ru}(\text{SMes})_4(4\text{-Etpy})]$ (**4**), $[\text{Ru}(\text{SMes})_4(4\text{-Bupy})]$ (**5**), $[\text{Ru}(\text{SMes})_4(3,5\text{-Me}_2\text{py})]$ (**6**), and $[\{\text{Ru}(\text{SMes})_4\}_2(\mu\text{-}4,4'\text{-bipy})] \cdot 0.5\text{CH}_2\text{Cl}_2 \cdot 0.5\text{C}_2\text{H}_5\text{OH}$ (**7**· $0.5\text{CH}_2\text{Cl}_2 \cdot 0.5\text{C}_2\text{H}_5\text{OH}$) have been

deposited with the Cambridge Crystallographic Data Center as supplementary publication nos. CCDC 1042039, 1042041–1042045, respectively. Copies of the data can be obtained free-of-charge on application to CCDC, 12 Union Road, Cambridge CB2 1EZ, UK [fax: (+44)1233–336-033; e-mail: deposit@ccdc.cam.ac.uk].

Disclosure statement

No potential conflict of interest was reported by the authors.

Funding

This work was supported by the Natural Science Foundation of China [grant number 21372007].

References

- [1] P.V. Rao, R.H. Holm. *Chem. Rev.*, **104**, 527 (2004).
- [2] T. Sriskandakumar, H. Petzold, P.C.A. Bruijninx, A. Habtemariam, P.J. Sadler, P. Kennepohl. *J. Am. Chem. Soc.*, **131**, 13355 (2009).
- [3] A. Romero-Pérez, A. Infantes-Molina, E. Rodríguez-Castellón, A. Jiménez-López. *Appl. Catal. B*, **97**, 257 (2010).
- [4] M.L. Zastrow, V.L. Pecoraro. *Coord. Chem. Rev.*, **257**, 2565 (2013).
- [5] Y. Yu, O.Y. Gutiérrez, G.L. Haller, R. Colby, B. Kabius, J.A. Rob van Veen, A. Jentys, J.A. Lercher. *J. Catal.*, **304**, 135 (2013).
- [6] X.M. Yang, X.N. Wang, J.S. Qiu. *Appl. Cat. A-General*, **382**, 131 (2010).
- [7] R.R. Chianelli, G. Berhault, B. Torres. *Cat. Today*, **147**, 275 (2009).
- [8] M. Kawano, H. Uemura, T. Watanabe, K. Matsumoto. *J. Am. Chem. Soc.*, **115**, 2068 (1993).
- [9] P.T. Bishop, A.R. Cowley, J.R. Dilworth, A.J. Saunders, J.G. Woolard-Shore. *Dalton Trans.*, 1267 (2006).
- [10] G. Belchem, J.W. Steed, D.A. Tocher. *J. Chem. Soc., Dalton Trans.*, 1949 (1994).
- [11] D. Sellmann, R. Ruf, F. Knoch, M. Moll. *Inorg. Chem.*, **34**, 4745 (1995).
- [12] R. Maiti, M. Shang, A.G. Lappin. *Chem. Commun.*, 2349 (1999).
- [13] S. Matsukawa, S. Kuwata, M. Hidai. *Inorg. Chem. Commun.*, **1**, 368 (1998).
- [14] S.A. Koch, M. Millar. *J. Am. Chem. Soc.*, **105**, 3362 (1983).
- [15] M.M. Millar, T. O'Sullivan, N. De Vries, S.A. Koch. *J. Am. Chem. Soc.*, **107**, 3714 (1985).
- [16] Q.F. Zhang, C.Y. Lai, W.Y. Wong, W.H. Leung. *Organometallics*, **21**, 4017 (2002).
- [17] R. Ye, A.-Q. Jia, Q. Ma, Q. Chen, W.-H. Leung, Q.-F. Zhang. *J. Organomet. Chem.*, **741/742**, 20 (2013).
- [18] *SMART and SAINT+ for Windows NT Version 6.02a*, Bruker Analytical X-ray Instruments Inc., Madison, Wisconsin, USA (1998).
- [19] G.M. Sheldrick. *SADABS*, University of Göttingen, Germany (1996).
- [20] G.M. Sheldrick. *SHELXTL Software Reference Manual*. Version 5.1, Bruker AXS Inc., Madison, Wisconsin, USA (1997).
- [21] G.M. Sheldrick. *Acta Crystallogr.*, **A 64**, 112 (2008).
- [22] S.P. Satsangee, J.H. Hain Jr, P.T. Cooper, S.A. Koch. *Inorg. Chem.*, **31**, 5160 (1992).
- [23] K. Matsuda, I. Yanagisawa, Y. Isomura. *Synth. Commun.*, **27**, 3565 (1997).
- [24] A.W. Addison, T.N. Rao. *J. Chem. Soc., Dalton Trans.*, 1349 (1984).
- [25] R. Prakash, A.W. Götz, F.W. Heinemann, A. Görling, D. Sellmann. *Inorg. Chem.*, **45**, 4661 (2006).
- [26] D. Sellmann, K. Engl, F.W. Heinemann, J. Sieler. *Eur. J. Inorg. Chem.*, 1079 (2000).
- [27] A.-Q. Jia, M. Chen, L.M. Shi, H.T. Shi, Q.-F. Zhang. *J. Coord. Chem.*, **67**, 3565 (2014).
- [28] Q.-F. Zhang, R.D. Adams, W.-H. Leung. *Inorg. Chim. Acta*, **359**, 978 (2006).
- [29] H. Yan, G. Süss-Fink, A. Neels, H. Stoeckli-Evans. *J. Chem. Soc., Dalton Trans.*, 4345 (1997).